Defining and determining the properties of the human sleep homeostat

Zavada, Andrei

Part II

Sleep Homeostasis

Chapter 4

A Method to Determine the Properties of the Homeostatic Component of Slow Wave Activity Regulation in Humans

Andrei Zavada, Domien G. M. Beersma, Marijke C. M. Gordijn, Serge Daan

Abstract

Sleep is considered a homeostatic (need-need reduction) process gated by a circadian pacemaker. The kinetics of the homeostatic process have been derived from the Slow Wave Activity (SWA, spectral power in the delta band) in the EEG. It is described by a pair of parameters. The "rise rate" determines the rate of sleep debt accumulation during wake, and the "gain constant" reflects the efficiency of SWA in dissipating sleep debt. These parameters define individual average levels of Process S in steady state and tolerance to sleep loss. We developed a method to estimate the properties of the homeostatic component, using an enhanced version of the model of Achermann et al (1993). This was applied to EEG recordings from central (C3A2) and frontal (FzA1) derivations taken in a series of sleep episodes (baseline night at habitual times, early afternoon nap, night awake, late afternoon nap, recovery night). The subjects were 9 early and 8 late chronotypes selected using the Munich Chronotype Questionnaire. Each subject completed the protocol 3 times. The gain constant was significantly smaller in Early than in Late group (C3A2: average 0.00579 and 0.00752; FzA1: 0.00592 and 0.00810 min^{-1}, respectively). This difference may be attributable to age differences between the groups, as the gain constant decreased significantly with age. The result implies that the the earlier timing of sleep with increasing age, and possibly also the tendency of certain individuals to advance sleep timing regardless of age, may be associated with a reduced efficiency of SWA in sleep debt dissipation.

4.1 Introduction

The two-process model of sleep regulation (Borbély, 1982; Daan et al., 1984) was inspired by the systematic dependency of SWA (Slow Wave Activity, spectral power in the 0.75–4.5 Hz range of EEG signal) on prior sleep and wakefulness. SWA declines on average in the course of sleep, and increases following extended wakefulness. The model successfully predicted SWA in naps as varying with prior wake time and the effect of naps on subsequent SWA in the next night (Dijk et al., 1987a). According to the model, SWA reflects the state of the homeostatic Process S, yielding a quantitative measure of what is commonly known as sleep debt or sleep pressure.

Properties of Process S alone can determine actual sleep timing in the model. It is possible that individuals vary in parameter values of this process and that their variation in sleep timing is attributable to Process S. This would then affect individual chronotype, even with invariant properties of the circadian component (Process C). Although the period and amplitude of Process C do obviously cause sleep to occur preferentially at a particular time (Duffy et al., 2001), or not to occur at inappropriate time (Daan et al., 1984), the contribution of Process S is certainly not negligible (Dijk and Czeisler, 1994, 1995). Figure 4.1 shows 2 simulations of the two-process model with the same phase and amplitude of Process C and identical initial conditions but different rise rates of Process S. This demonstrates that a smaller rise rate will result in later sleep timing and shorter sleep. Similarly, a slower decay rate will result in later sleep timing and in longer sleep. There are indications in the literature (Kerkhof, 1991) showing a slower decline of SWA in late chronotypes as compared to early chronotypes. Such information is not available for the rise rate of S during wakefulness. For these reasons, it is interesting to compare the rise rates of S in subjects characterized through age or by differences in sleep timing as demonstrated in a chronotype survey.

The level of Process S increases during wakefulness, as a saturating exponential function of time: $S(t) = 1-(1-S_0)\cdot\exp(-t/\tau_r)$, where t is time (h) into wakefulness and τ_r (h) is the inverse rise rate of S (Daan et al., 1984). Indirect experimental evidence suggests that the actual course of S approximates this equation rather accurately, suggesting that the state of wakefulness is homogeneous with respect to the rise rate of S (Dijk et al., 1987a). In sleep, the instantaneous rate of decay of S is proportional to the intensity of SWA (Dijk et al., 1987b;

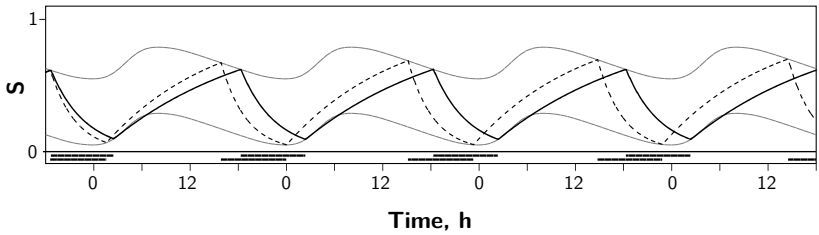

Figure 4.1 Displacement of sleep timing can be achieved by varying rise rate of Process S alone. The skewed sine waves represent the circadian Process C, common for both simulations. Confined between those are the simulated courses of Process S, differing only in the rise rate: 18.20 h (solid line) and 13.65 h (dotted line). Respective sleep periods (indicated below as thick solid lines) stabilize by the 3rd cycle, the former (above) lasting 8.1 h with midpoint at 4:19 h, and the latter (below) being 9.7 h long and centring at 2:42 h. For equations, see Daan et al. (1984).

Achermann et al., 1993), which is highly variable given the recurrent NREM–REM cycle and overall dynamics of individual sleep.

The sleep EEG SWA was initially proposed as a neurophysiological substrate for Process S (Borbély, 1982). Since the publication of the two-process model several authors have demonstrated that SWA at the beginning of sleep indeed almost exclusively depends on prior time awake, not on circadian phase (Dijk et al., 1987a; Cajochen et al., 2002).

While estimation of the rise rate of Process S is relatively simple and straightforward (requiring a minimum of three SWA data points; see Borbély's (1982) classic example), issues emerge when exponential course fitting is done to the inherently irregular SWA profile during sleep. The global course of S during sleep, when inferred from the course of SWA and averaged over nights and subjects, indeed appears roughly exponential. For individual nights, the ultradian component (the NREM–REM cycle) creates difficulties for fitting the course of S to the actual SWA profile. Rather important, in addition, is the relationship between the highly variable SWA and the abstract parameter S, which by definition is reflected in SWA. The existence of such relationship immediately suggests that S and SWA, although obviously interdependent, follow separate courses. And conversely, once the sleep debt dissipation must be a gradual process, spanning across

several NREM–REM cycles, there must be some mediating factors to buffer the irregularities of SWA and so to ensure the gradual decline of S.

One interesting attempt to accommodate the incongruity between S and SWA can be found in Dijk et al. (1987b), in which paper sleep dynamics is investigated in a selective sleep deprivation experiment. The authors reach one conclusion that has a bearing on the relationship between S and SWA, namely, that SWA reflects the rate of decay of S rather than the level of S proper. This can be viewed as a precursor of the gain constant of Achermann et al (1993). However, there is no clear separation of S from SWA yet. In fine detail, several dynamic components govern the course of SWA during sleep (Achermann et al., 1993). In particular, Achermann et al included provisions in their model for the time lag between sleep onset and the actual peak of SWA (where the level of S is at its maximum), as well as for the presence of REM sleep. These dynamical properties were included in mathematical approximations in which the course of S is derived *in a continuous manner* from a set of basic sleep parameters and a hypnogram. Achermann et al (1993) did this by reconstructing the SWA profile as an intermediate step, then matching it to the real EEG data and modifying the parameters of the model according to the deviation between the simulated and real SWA courses. We adopted their approach and expanded it by fitting the model to a series of multiple sleep episodes. The periods of intervening wakefulness enabled us to determine the rise rate during wakefulness along with the decay rate and several other parameters of the model. The rise rate was necessarily assumed invariant in Achermann's work, whose datasets did not include sufficiently long intervals of wakefulness to estimate the rise rate.

In earlier publications (Dijk and Beersma, 1989; Kerkhof, 1991), using a classical way of fitting an exponential curve to the NREM–REM-cycle averaged SWA values, authors have already observed differences between Early and Late human chronotypes. We demonstrate the method and show how its parameter estimates vary with both chronotype and age in ways suggesting that part of the interindividual variance in chronotype may indeed be related to Process S rather than to Process C alone.

4.2 Materials and Methods

4.2.1 Subjects

For the data to be analysed we exploited EEG records obtained in a study on the effects of light at different circadian phases in human extreme early and late chronotypes. Subjects were selected from the database of over 5100 respondents to the Munich Chronotype Questionnaire, used in a survey of sleeping habits in the Netherlands (Zavada et al, 2005). We defined two extreme groups on the basis of age-corrected free-day mid-sleep time (MSF_{ac}, introduced by (Roenneberg et al., 2003). Age correction was done as follows. For subjects over 20 y.o.:

$$MSF_{\mathrm{ac}} = MSF - (-0.12206 \cdot (age - 30) + 0.00096571 \cdot (age^2 - 900)),$$

and for ages ≤ 20 years, an intermediate term was computed:

$$MSF_{20} = MSF - (0.83476 \cdot (age - 20) - 0.019844 \cdot (age^2 - 400)),$$

$$MSF_{\mathrm{ac}} = MSF_{20} - 0.737745$$

Subjects with MSF_{ac} in the lower 15 % of the value range formed the Early group, and those with MSF_{ac} in the upper 15 % of the range were in the Late group.

Prospective subjects were sent a message describing the purpose of the experiment and reasons for us to select the addressee. If consenting and meeting conditions of absence of current medical treatment and of sleep disturbances, they were invited for an interview. We selected 19 subjects for participation in the study. Three weeks prior to the agreed start of the experiment, each participant was instructed to wear an Actiwatch® to log their factual sleep times. We finally recruited 8 subjects (6 females, 2 males, mean age 21.9 ± 2.36 yr, range 18–26 yr) into the Late group and 9 subjects (all females, mean age 36.1 ± 13.14 yr, range 21–58 yr) into the Early group.

Subjects were paid for their efforts. The study was approved by the Medical Ethical Committee of the University Medical Center in Groningen, The Netherlands.

4.2.2 Protocol

The experimental protocol included 3 conditions, called Dim Light, Morning Light and Evening Light. The conditions differed with re-

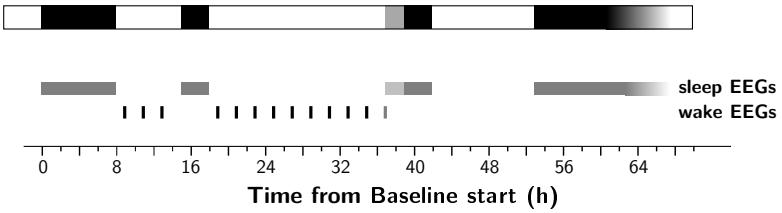

Figure 4.2 Experimental protocol. Upper bar shows scheduled sleep in black; a grey 2-h extension in front of the 2nd nap indicates that such extension was allowed for subjects in the Early group, but the Late group had only a 3-h nap. Both groups slept *ad libitum* in the Recovery night, *i.e.,* without a fixed sleep end.

spect to environmental lighting. Most of the times subjects stayed in dim light, except that in the Morning Light and in the Evening Light conditions, they were exposed to bright light for 4 h. Since the light is supposed to only affect the circadian pacemaker, not process S, we have analysed the 3 conditions as if they were identical. Each condition had four sleep episodes (Fig. 4.2): baseline sleep (0–8.5 h), which was scheduled at the subject's habitual hours as logged by the Actiwatch, 1st nap (15–18 h), 2nd nap (39–42 h in the Late group, 37–42 h in the Early group), and recovery sleep (53 h until spontaneous awakening). The times in parentheses refer to the hours after lights-out at the start of the baseline sleep episode. In real clock time the timing of the sleep episodes varied according to the habitual sleep timing of the subjects as established by prior actimetry during 3 weeks. The baseline night was therefore centered around the individual habitual mid-sleep time. Subjects were briefly awoken every 2 h during baseline and recovery nights for the collection of a saliva sample.

The deprivation of sleep during the second night was needed for the proper administration of the light treatment to assess circadian resetting properties (Chapter 3). We experienced that the Early subjects had often severe difficulties in staying awake during this prolonged wake episode. Indeed, one of the first Early subjects quit the experiment failing to maintain wakefulness between the 1st and 2nd nap. We then decided to reduce the span between the naps in the Early group by 2 hours and to allow them 2 extra hours of sleep. One subject (#21) was allowed to begin her Dim Light condition's 2nd nap at 36 h due to overwhelming sleepiness, sleeping subsequently for 6 hours.

Table 4.1 Subject data and sleep statistics (group averages ±SD). MSF (h) is the self-reported free-day mid-sleep time, MSF_{ac} (h), same, age-corrected. Habitual sleep times (clock hours) from 3 weeks preceding admission as logged by Actiwatch.

	Early	Late	p
Age	36.1 ± 13.1	21.9 ± 2.4	0.01
MSF	2.74 ± 0.9	8.02 ± 1.2	<0.001
MSF_{ac}	2.94 ± 0.7	7.48 ± 1.2	<0.001
Habitual sleep onset	22.7 ± 1.6	3.02 ± 0.9	<0.001
Habitual mid-sleep	2.99 ± 1.2	6.95 ± 1.1	<0.001
Habitual sleep end	7.28 ± 1.1	10.9 ± 1.3	<0.001
Habitual sleep duration	8.59 ± 1.3	7.88 ± 0.9	0.20
MEQ score	59.8 ± 10.0	26.5 ± 2.1	<0.001

For subjects' age, reported and age-corrected MSF, and habitual sleep times, see Table 4.1. Sleep statistics collected during the experiment are presented in Table 4.2.

4.2.3 EEG measurements

Sleep EEGs from central (C3A2) and frontal (FzA1) derivations were recorded in all sleep episodes, along with two EOGs and a submental EMG. The data were low-pass filtered at 30 Hz with a time constant of 1 s, and subsequently sampled at 128 Hz. Sleep stages were manually scored by 30-s pages following Rechtschaffen and Kales (1968) assisted by the EEG scoring program Vitascore® (TEMEC Instruments, Kerkrade, The Netherlands). Pages scored as NREM Stage 1–4 and REM were included in the power spectrum analysis. Power spectra were obtained for the range 0–32 Hz with 0.25 Hz resolution, using fast Fourier transformation routines with a Hanning window size of 4 s.

4.2.4 Implementation of the model

The model we used to describe the sleep structure is that first proposed by Achermann et al (1993), with modifications to adapt it to our experimental protocol. Given the REM, NREM and WAKE scores and the starting value of slow-wave activity at time 0 (SWA_0), it employs two differential equations to reconstruct the course of SWA

Table 4.2 Sleep statistics (group averages). Start ("at") is given on the absolute protocol timeline; start and length ("len") in hours, efficiency ("eff") as percentage of time spent in sleep (NREM Stages 1–4 or REM) out of total time in bed.

Group	Baseline			1st nap		
	at	len	eff	at	len	eff
Late	0	8.5	58.2	14.8	3.0	58.0
Early	0	8.5	53.6	14.6	3.0	47.7
	2nd nap			Recovery		
Late	38.7	3.0	68.5	53.1	6.2	56.6
Early	36.0	5.3	52.0	53.0	5.4	52.8

and that of S along the timeline, as follows:

$$\begin{aligned} \mathrm{d}S/\mathrm{d}t &= -gc \cdot SWA \cdot !\mathrm{WT} + (S_\mathrm{U} - S) \cdot rs, \qquad (4.1) \\ \mathrm{d}SWA/\mathrm{d}t &= rc \cdot SWA \cdot (S/S_\mathrm{U})(1 - SWA/S) \cdot !\mathrm{WT} \\ &\quad - fc_\mathrm{R} \cdot (SWA - SWA_\mathrm{L}) \cdot \mathrm{REMT} \\ &\quad - fc_\mathrm{W} \cdot (SWA - SWA_\mathrm{L}) \cdot \mathrm{WT} \qquad (4.2) \end{aligned}$$

where SWA and S are instantaneous simulated values expressed as percentage of the mean SWA over all baseline pages scored as NREM; SWA_L is the lower asymptote for SWA, defined as 95 % of the lowest SWA observed in all REM pages of baseline; S_U is the upper asymptote of S; rc, gc, rs, fc_R and fc_W are sleep parameters described in Table 4.3; WT = 1 on wake, else 0; REMT = 1 during and from t_a min before REM sleep, to allow for the SWA drop caused specifically by REM, and for t_p min after a REM episode end, because effects of REM interfering with SWA are still apparent for some time; t is time (min). The operator '!' is logical negation (thus $!x = 0$ for any $x \neq 0$, and $!0 = 1$).

Note that there is no specific decay counterpart for the rise rate of Process S (rs): indeed, as long as dissipation of sleep pressure is the direct effect of SWA, the irregularity and variable strength of SWA across a sleeping episode will likewise result in varying decrements in S. This is in contrast to the homogeneous S-elevating quality of wakefulness, where a constant rise rate can be defended. There is evidence

Table 4.3 Parameters of the model. Initial values derived by Achermann et al. (1993) for the 'normal' state. For limits, see Table 5.1 on page 77.

Param.	Unit	Description	Tuned	Initial value
rc	min^{-1}	SWA rise constant	yes	0.283
fc_{R}	min^{-1}	SWA fall constant triggered by REM	yes	0.236
fc_{W}	min^{-1}	SWA fall constant triggered by Wake	no	1
gc	min^{-1}	Gain constant	yes	0.835×10^{-2}
S_0	%	Level of S at sleep onset	yes	300
S_{U}	%	Upper asymptote of S	yes*	400
t_{a}	min	Anticipated effect of REM on SWA	no	6
t_{p}	min	Extension of effect of REM on SWA	no	3
rs	min^{-1}	Rise rate of S	yes	0.917×10^{-3}

(*) S_{U} is tied to rs and not tuned independently:
$S_{\text{U}} = (S_0 - S_{\text{baseline\_end}} \cdot \exp(-t \cdot rs))/(1 - \exp(-t \cdot rs))$,
t being here 24 h less the duration of the baseline night.

that variations in the rate of sleep debt build-up do not correlate with variation in mental workload (De Bruin et al., 2002).

The data Achermann and colleagues (1993) used to develop their implementation of the model included a single night for each subject, *i. e.,* without long periods of sustained wakefulness separating sleep episodes. With those data, it was not possible to quantify the rise rate of S during wakefulness. Achermann and co-workers took the value deduced from sleep deprivation experiments as calculated by Daan et al. (1984). Our study included three long intervals of wakefulness, and we could therefore make the rise rate a free parameter.

The original Achermann et al's equations, however, needed to be modified to enable an accurate estimation of the rise rate. The term $-gc \cdot SWA$ never equals 0 due to simulated SWA never falling below SWA_{L}. During wake, this would result in an additional decrement to S caused by nonexisting SWA, eventually preventing S at time 24 h from reaching the value S had at time 0. Since Achermann et al's datasets had no sizable wake intervals, the side effects of such decrements passed virtually unnoticed. As the condition $S_0 = S_{24}$ is required for the derivation of the rise rate (see note under Table 4.3), we cancel this term except during NREM. Additionally, in the second

equation, we cancel the term $rc \cdot SWA \cdot (S/S_U) \cdot (1 - SWA/S)$ during wake as well; but the effects of this modification appeared marginal.

Our method of fitting the model equations comprises three nested loops, the innermost of which iterates along the timeline, page by page (dt thus equals 30 s), to produce an SWA profile for a given set of parameter values. This is compared with the empirical SWA, and the fit is calculated as a sum of squares of the differences between these in all SWA-containing pages. At the end of the iteration one of the tunable parameters is given a fixed increment of random sign and the iteration is repeated. The fit is then compared to that from the previous run, and an increase or decrease in the deviation is used to retain or reverse the direction of the 'drift'; this is done for each of the parameters, in random order. When a total of 400 iterations are completed, the resulting set of parameter values and the fit value are stored, again to be compared to the corresponding values from the previous iteration cycle ('stride'). Such strides, each resuming at parameter values where the preceding stride left off, are repeated until the improvement of the fit between two consecutive strides is less than 0.05 % and no parameter has a drift on the last stride greater than 0.05 % of its initial value. Finally, the entire procedure, starting from randomization of initial parameters, was repeated 4 times and the best-fit outcome was chosen.

The model fitting procedure described above was designed to run on data from a single condition. Since all but 3 of our subjects had all three conditions completed, we further implemented a combined model fitting procedure. This included multiple timelines at once and yielded parameter tuning such that the variance on the sum of all fits is minimal. Parameters, here, would in each condition drift variable distances during a stride: therefore, at checkpoints between strides each parameter receives an average drift value from all concurrent conditions. In this setup, however, S_0 is maintained as a separate variable in each condition as subjects may approach different conditions with different values of S, and so also varies S_U (see note under Table 4.3). The whole fitting procedure for a single subject in three conditions typically took *ca* 40 min on a Pentium III PC.

4.2.5 Statistics

Individual SWA profiles in each condition were normalized to the average SWA in the baseline night. Model fitting parameters were com-

pared between groups using a t-test; to estimate the effect of age and MSF_{ac} on the parameters, a multiple regression analysis was performed with factors age, MSF_{ac}, and the combination of $age \times MSF_{\mathrm{ac}}$.

Computational tasks were programmed in Octave, version 2.9.4 (`www.octave.org`) and C++ using librasch (`www.librasch.org`) for reading edf files. Statistics were obtained in *R: A language and environment for statistical computing*, version 2.2.0 (`www.r-project.org`).

4.3 Results

Fourteen subjects (7 Early and 7 Late) completed all three conditions. One Early Subject completed 2 conditions. Two more subjects (one Early, one Late) completed only the first (DIM) condition. A few sleep episodes had to be discarded due to artefacts. Overall, the combined model-fitting could be applied to 14 Subjects (7 Early, 7 Late). Where a complete SWA profile was available for only one condition (3 cases), combined model fitting was replaced by a simpler, single-condition procedure. All SWA profiles from the Dim Light condition are given in Fig. 4.3.

One example of the outcome of model fitting is presented in Fig. 4.4. It demonstrates empirical SWA, and as reconstructed by the model, along with the time course of S computed in the fitting procedure. Table 4.4 summarizes the resulting parameters of fitting the model to the individual data averaged per group, as well as their interindividual standard deviation. We found no significant differences between the early and late groups in their average rs (rise rate of S), in fc_{R} (SWA drop in REM) nor in rc (SWA rise constant), neither in central nor in frontal EEG derivations. The only parameter whose average value differed significantly between groups in both derivations was the gc parameter. This gain constant, the estimated relationship of SWA to the rate of decay in S, was on average 30 % larger in the C3A2 and 37 % larger in the FzA1 derivation in Late types than in Early types. Both differences were significant at the $p < 0.05$ level (two tailed t-test).

We can compare the sleep parameters of our subjects to those Achermann et al (1993) established for subjects not selected for extreme chronotype ('Initial values' in Table 4.3). The Achermann's value of the gain constant ($0.835 \times 10^{-2}\,\mathrm{min}^{-1}$) is close to the value we find for the average late subject. The rise rate reported by Acher-

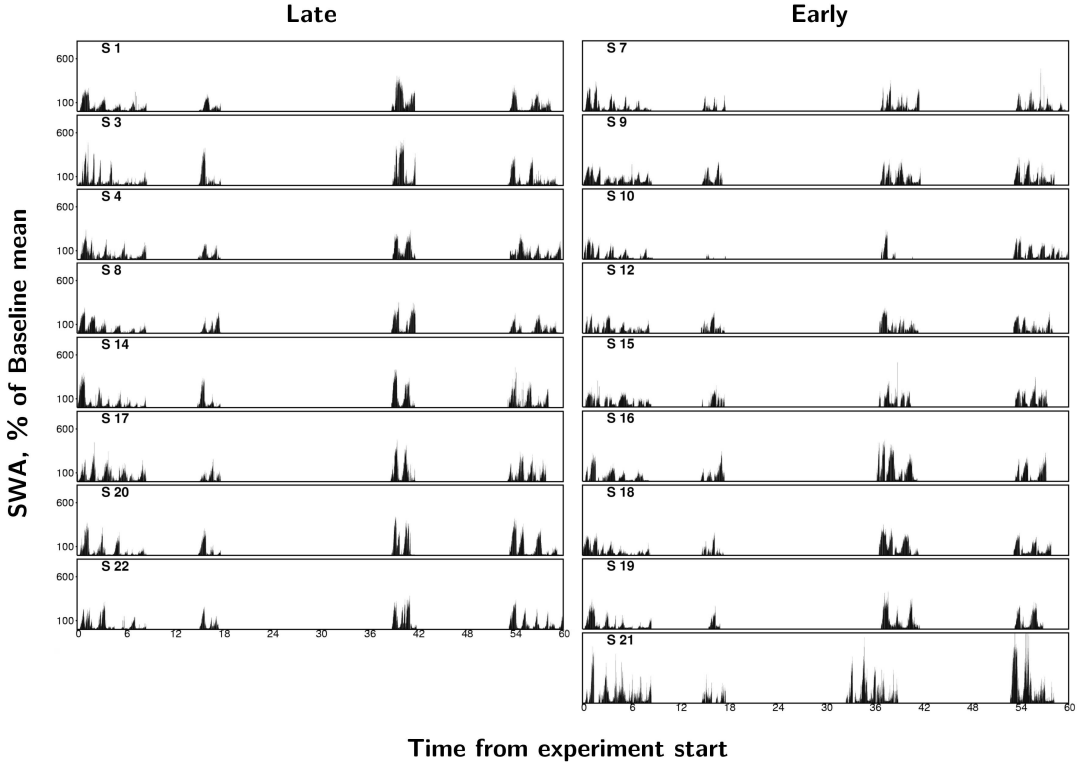

Figure 4.3 SWA profiles of all subjects in the Dim Light condition, normalized to individual Baseline average.

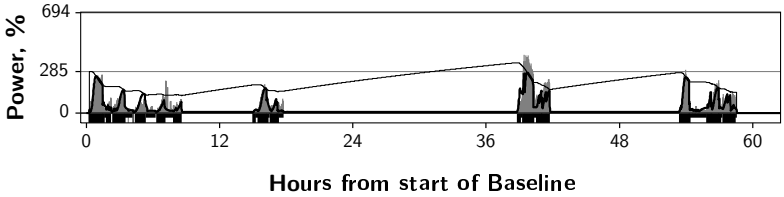

Figure 4.4 Model fitting of one of the subjects, showing the original SWA profile (central derivation, grey area) with simulated SWA on top (thick solid line) and the reconstructed course of Process S (thin solid line), along the protocol timeline. Solid bars under the zero line indicate REM sleep (half-height bars) and NREM sleep (full-size bars). SWA (%) is normalized to its average in the baseline night. The ticks on the *y*-axis are the starting value of S (at 285 % in this example) and the S asymptote (at 694 %). Note that S in Achermann's simulations is codimensional with SWA, and so is expressed in %. It can be converted into the original representation of Borbély (1982) and Daan et al. (1984) by dividing over its upper asymptote, S_{U}, which is a free parameters in our simulations.

mann, who in turn used the value previously computed by Daan et al (1984), is $0.9167 \times 10^{-3}\,\mathrm{min}^{-1}$, which is close to our average early subject.

The levels of S (for an individual example of the course of S, see Fig. 4.4) computed at the beginning and end of each sleep episode, averaged within groups, are collected in Table 4.5. The S levels at the beginning and end of the sleep episodes in baseline and first nap were lower in Late than in Early types, in both EEG derivations. Levels of S are not statistically compared in the remaining sleep episodes, as the timing and duration of the 2nd nap is different between groups. Still, the differences between groups were more conspicuous in the central derivation than in frontal derivation, and were always higher on average in the early than in the late group. None of the values by itself differed significantly between the groups, though, except the level of S at the end of the 1st nap. This single significance can not be taken seriously as it would readily disappear with Bonferroni adjustment.

In view of the unequal breakdown of ages in the two groups, we carried out a multiple regression analysis to determine the association of sleep parameters with age and chronotype (Midsleep on Free days or MSF_{ac}). Table 4.6 lists the F, p and R^2 values of the effects *age*, MSF_{ac}, and *age* $\times$ MSF_{ac} on the gain constant. This analysis

Table 4.4 Model fitting: resulting parameters. $n = 8$ in Late group, 9 in Early group. The p values are for a two-tailed t-test.

	$rs \times 10^3$	fc_{R}	rc	$gc \times 10^2$
Central				
Late types	0.52 ± 0.24	0.31 ± 0.05	0.49 ± 0.18	0.75 ± 0.10
Early types	0.88 ± 0.62	0.29 ± 0.04	0.42 ± 0.11	0.58 ± 0.19
p	0.129	0.349	0.304	0.038
Frontal				
Late types	0.58 ± 0.29	0.32 ± 0.06	0.48 ± 0.17	0.81 ± 0.12
Early types	0.67 ± 0.40	0.30 ± 0.04	0.52 ± 0.21	0.59 ± 0.23
p	0.607	0.342	0.640	0.047

shows that the association of gc with chronotype can be attributed to differences in average age between the two groups.

4.4 Discussion

4.4.1 Reliability in estimation of principal sleep parameters

The application of Achermann's version of the two-process model to a series of EEG recordings proved usable in determining the two principal parameters of the homeostatic component, the rise rate of Process S and the gain constant. This approach assumes that individual sleep parameters do not vary over the time interval under consideration. Generally, its design allows for any irregular series of sleep and wake intervals from which to reconstruct the course of Process S. The gain constant can immediately be determined from any SWA profile, while estimation of the rise rate is only possible from profiles longer than 24 h, and in which at least two major sleep episodes occur.

Conceptually, the rise rate of S during waking refers to the increase of sleep need dependent on wakefulness. No distinction is made between different behavioural or conscious states during waking, precisely as in the original proposition of the two-process model of sleep regulation (Daan et al., 1984). This assumption is consistent with the absence of major influences of heavy mental work load on SWA (De Bruin et al., 2002), and the interpretation of the rise rate of S is

Table 4.5 Model fitting: levels of S (normalized to S_{U}) at the beginning and end of sleep episodes, group means. $n = 8$ in Late group, 9 in Early group. The p values are for a two-tailed t-test. *Average* is obtained from the entire timeline; *Amplitude* is the difference between S maximum and minimum. See Fig. 4.4 for an example (where S is the thin solid line running over and through SWA peaks).

	S									
	Baseline		1st nap		2nd nap		Recovery		Average	Amplitude
	Start	End	Start	End	Start	End	Start	End		
Central										
Late types	0.55	0.31	0.42	0.35	0.63	0.40	0.55	0.35	0.44	0.43
Early types	0.69	0.41	0.55	0.49	0.75	0.50	0.69	0.48	0.57	0.34
p	0.093	0.096	0.091	0.050						
Frontal										
Late types	0.56	0.31	0.42	0.36	0.64	0.41	0.56	0.36	0.45	0.44
Early types	0.62	0.37	0.48	0.43	0.68	0.45	0.62	0.44	0.51	0.32
p	0.509	0.436	0.480	0.309						

Table 4.6 Effect of age and MSF_{ac} on the gain constant, in central and frontal derivations.

Derivation	age			MSF_{ac}			$age \times MSF_{\mathrm{ac}}$		
	$F_{1,15}$	p	R^2	$F_{1,15}$	p	R^2	$F_{2,14}$	p	R^2
Central	8.378	0.011	0.358	2.818	0.114	0.158	4.011	0.042	0.364
Frontal	9.658	0.007	0.392	2.904	0.109	0.162	4.586	0.029	0.396

unaltered in Achermann's elaboration. The relevance of Achermann's work concerns the mechanism of S dissipation. Thus, the gain constant used by Achermann et al (1993) as well as in the present study, is not identical to the decay rate of S as defined in the original two process model. The difference is that the gain constant describes the direct relationship between SWA and the instantaneous decay rate of Process S (*cf.* the conclusion of Dijk et al. (1987b), whereas the original decay rate is an all-night constant, derived from averaged per NREM episode SWA data. While we assume that the gain constant is indeed constant per individual, the classical decay rate may well depend on the quality of sleep and thus vary from one sleep episode to another. If it is difficult to obtain deep sleep at certain phases, this would likely yield a smaller decay rate in the classical sense, while Achermann's method would still produce an invariant gain constant: absence of high values of SWA *per se* can only affect gain constant estimation indirectly, through increasing error.

The quality of sleep itself influences the accuracy of estimation of the rise rate. The reason is that the expression of SWA during a specific sleep episode is no longer solely determined by the need for sleep that has accumulated during prior wakefulness, but also by the quality of the sleep episode. Even though both naps in our protocol were placed approximately at the time of the afternoon "post-lunch dip", subjects may well have differed in their ability to maintain an adequate SWA intensity. SWA expression in the naps could further be affected by the strength of intrusions of REM sleep. These factors could disrupt the course of SWA that would otherwise be appropriate to discharge its homeostatic function, affecting the accuracy of estimation of the rise rate.

The value of the rise rate taken as representing a 'normal' subject in Achermann et al. (1993) is on the early side when compared against our subjects, whereas his computed value of the gain constant places Achermann's 'normal' type among our extreme late types. This discrepancy can be explained as follows. Achermann et al did not compute the rise rate, instead having it fixed at a value previously derived in Daan and Beersma (1983) and Daan et al. (1984). The latter authors had taken a simpler approach and fitted an exponential curve to the raw SWA profile, whereas Achermann's approach considers REM intrusions and SWA build-up latency and is dependent on supplied sleep scores. Being more flexible by design, this method is at the same time dependent on several new factors. Unavoidably, inclusion of new parameters will influence the exact rise rate estimation, which eventually is likely to differ from the 'classical' rise rate of Daan et al. (1984). As the classical decay rate is superseded by the gain constant, one and the same steady state could equally well be described by the pair decay rate – rise rate, in classical terms, and by the pair gain constant – rise rate, in Achermann's terms, but the invariant term (rise rate) can be numerically different, which we speculate has taken place in Achermann's and our simulations.

In this study we have assumed that individual sleep homeostat parameters remain the same for the entire experimental timeline. In a study by Werth et al. (1996), Achermann's method predicted a higher SWA for a daytime nap as well as for the night following as compared to actual observations. This can indicate that at inappropriate times, SWA regulation can be better simulated by parameters more or less different from those determined for the baseline conditions. In another experiment using Achermann's model, we found that the gain constant in recovery tends to be lower than in baseline. An investigation of properties of the sleep homeostat under strain can be promising.

4.4.2 Evidence for frontal predominance

Differences in gain constant (higher levels found in frontal derivations compared to central derivations) suggest a trend for SWA to be more efficient in dissipating Process S in frontal than in central areas. This can be interpreted in conjunction with the frontal predominance, or "hyperfrontality", established for SWA (Werth et al., 1997; Finelli et al., 2001b; Cajochen et al., 1999). Indeed, a larger SWA rebound after sleep deprivation in frontal areas reported by Cajochen et al. (1999)

implies a larger increase in the level of Process S between baseline and recovery sleep. This is achieved with a smaller rise rate, because otherwise, high rise rates would cause the system to approach the upper asymptote with a high rate. As a result, S will be close to the upper asymptote at the end of a normal day, and not much of an additional increase can be expected from longer intervals of wakefulness. We are currently analyzing this aspect in more detail.

4.4.3 A causal link between parameters of sleep homeostat and chronotype?

As seen in a simple simulation (Fig. 4.1), sleep duration, average level of S and sleep timing are all dependent in the two-process model on a particular combination of the rise rate and "decay rate" (this decay rate is roughly inversely related to the gain constant). An increase in the rise rate leads to an advance of sleep, accomplished primarily through advance of sleep onset, thus effectively shaping the early chronotype. To retain the same sleep duration, an increase in the rise rate must be accompanied by an increase in the "drop rate".

A recent paper (Mongrain et al., 2006a) has sought to establish this link between sleep homeostat properties and chronotype. Operating on the average SWA values in the first four NREM–REM cycles, the authors reported a higher amplitude of SWA (again, most notably in the frontal derivation) in morning than in evening types, which agrees well with our data analysis. No abstraction was made from raw SWA to the Process S, but Mongrain et al's results are nonetheless in good agreement with the prediction of the model as well as with the trend observed in our data (Table 4.4). The same applies to a study by Kerkhof (1991), showing a faster decline of SWA across the sleep episode in early types.

In our own experiment, age has obscured the conclusions on rise rate and gain constant differences between chronotypes. As a consequence of the subject selection process that focused on chronotype, we ended up with early types that are on average older than the late types. Age has a profound influence on sleep dynamics (Dijk and Duffy, 1999; Dijk et al., 2000; Cajochen et al., 2006), phase relationship between sleep timing and properties of the circadian system (Duffy and Czeisler, 2002), as well as on chronotype (Roenneberg et al., 2004a). We cannot discriminate between age or chronotype as the primary explanatory factors behind the observed differences. Statistically, the

chronotype seems to be more influenced by age, in line with the evidence that midsleep time shifts forward with increasing age during adulthood (Duffy and Czeisler, 2002; Roenneberg et al., 2004a). It is not excluded that both age-dependent and age-independent variance in gain constant contribute to the variance in chronotype. At most, the study by Cajochen et al. (2006) demonstrates that homeostatic aspects of sleep regulation do not depend very strongly on age, suggesting that the variance in chronotype might be the crucial factor in our study.

The model we have presented in this article is an enhanced version of the two-process model formalization originally proposed by Achermann et al. (1993). One particular advance of our own is in the ability to estimate the rise rate of Process S, albeit with less accuracy than the gain constant, and only in studies containing 2 or more intervals of wakefulness are included, due to the exponential shape of the time course of Process S during wakefulness. The temporal characteristics of the rise rate require that such intervals last for quite some time (at least in the order of 10 hours), otherwise the fitting procedure will not strongly depend on the value of the rise rate, and reliable estimates cannot be obtained. Such data with EEGs around long wake episodes do not abound in the literature. They are necessary for a quantitative evaluation of the whole homeostatic sleep control process, as may be crucial for the explanation of at least part of the variance in human circadian entrainment.

4.5 Acknowledgements

AZ is supported by the Ubbo Emmius scholarship from the University of Groningen. The experiment was carried out as part of the BrainTime project (EC 5th framework grant QLG3-CT-2002-01829).